

Neutrino Physics with an Opaque Detector

A. Cabrera^{*1,9,10}, A. Abusleme¹⁵, J. dos Anjos^{†3}, T. J. C. Bezerra¹⁸, M. Bongrand⁹, C. Bourgeois⁹, D. Breton⁹, C. Buck¹², J. Busto⁶, E. Calvo⁵, E. Chauveau⁴, M. Chen¹⁶, P. Chimenti¹¹, F. Dal Corso¹³, G. De Conto¹¹, S. Dusini¹³, G. Fiorentini^{7a,7b}, C. Frigerio Martins¹¹, A. Givaudan¹, P. Govoni^{2a,2b}, B. Gramlich¹², M. Grassi^{1,9}, Y. Han^{1,9}, J. Hartnell¹⁹, C. Hugon⁶, S. Jiménez⁵, H. de Kerret^{†1}, A. Le Nevé⁹, P. Loaiza⁹, J. Maalmi⁹, F. Mantovani^{7a,7b}, L. Manzanillas⁹, C. Marquet⁴, J. Martino¹⁸, D. Navas⁵, H. Nunokawa¹⁴, M. Obolensky¹, J. P. Ochoa-Ricoux^{8,15}, G. Ortona²⁰, C. Palomares⁵, F. Pessina¹⁴, A. Pin⁴, M. S. Pravikoff⁴, M. Roche⁴, B. Roskovec⁸, N. Roy⁹, C. Santos¹, A. Serafini^{7a,7b}, L. Simard⁹, M. Sisti^{2a,2b}, L. Stanco¹³, V. Strati^{7a,7b}, J.-S. Stutzmann¹⁸, F. Suekane^{*§1,17}, A. Verdugo⁵, B. Viaud¹⁸, C. Volpe¹, C. Vrignon¹, S. Wagner¹, and F. Yermia¹⁸

¹APC, CNRS/IN2P3, CEA/IRFU, Observatoire de Paris, Sorbonne Paris Cité University, 75205 Paris Cedex 13, France

^{2a}Università di Milano-Bicocca, I-20126 Milano, Italy

^{2b}INFN, Sezione di Milano-Bicocca, I-20126 Milano, Italy

³Centro Brasileiro de Pesquisas Físicas (CBPF), Rio de Janeiro, RJ, 22290-180, Brazil

⁴CENBG, UMR5797, Université de Bordeaux, CNRS/IN2P3, F-33170, Gradignan, France

⁵CIEMAT, Centro de Investigaciones Energéticas, Medioambientales y Tecnológicas (CIEMAT), E-28040 Madrid, Spain

⁶Aix Marseille Univ, CNRS/IN2P3, CPPM, Marseille, France

^{7a}Department of Physics and Earth Sciences, University of Ferrara, Via Saragat 1, 44122 Ferrara, Italy

^{7b}INFN, Ferrara Section, Via Saragat 1, 44122 Ferrara, Italy

⁸Department of Physics and Astronomy, University of California at Irvine, Irvine, California 92697, USA

⁹LAL, Univ. Paris-Sud, CNRS/IN2P3, Université Paris-Saclay, Orsay, France

¹⁰LNCA Underground Laboratory, CNRS/IN2P3 - CEA, Chooz, France

¹¹Departamento de Física, Universidade Estadual de Londrina, 86051-990, Londrina – PR, Brazil

¹²Max-Planck-Institut für Kernphysik, 69117 Heidelberg, Germany

¹³INFN, Sezione di Padova, via Marzolo 8, I-35131 Padova, Italy

¹⁴Department of Physics, Pontifícia Universidade Católica do Rio de Janeiro, Rio de Janeiro, RJ, 22451-900, Brazil

¹⁵Pontificia Universidad Católica de Chile, Santiago, Chile

¹⁶Department of Physics, Engineering Physics & Astronomy, Queen's University, Kingston, Ontario K7L3N6, Canada

¹⁷RCNS, Tohoku University, 6-3 AzaAoba, Aramaki, Aoba-ku, 980-8578, Sendai, Japan

¹⁸SUBATECH, CNRS/IN2P3, Université de Nantes, IMT-Atlantique, 44307 Nantes, France

¹⁹Department of Physics and Astronomy, University of Sussex, Falmer, Brighton BN1 9QH, United Kingdom

²⁰INFN, Sezione di Torino, I-10125 Torino, Italy

August 9, 2019

The discovery of the neutrino by Reines & Cowan in 1956 revolutionised our understanding of the universe at its most fundamental level and provided a new probe with which to explore the cosmos. Furthermore, it laid the groundwork for one of the most successful and widely used neutrino detection technologies to date: the liquid scintillator detector. In these detectors, the light produced by particle interactions propagates across transparent scintillator volumes to surrounding photo-sensors. This article introduces a new approach, called LiquidO, that breaks

with the conventional paradigm of transparency by confining and collecting light near its creation point with an opaque scintillator and a dense array of fibres. The principles behind LiquidO's detection technique and the results of the first experimental validation are presented. The LiquidO technique provides high-resolution imaging that enables highly efficient identification of individual particles event-by-event. Additionally, the exploitation of an opaque medium gives LiquidO natural affinity for using dopants at unprecedented levels. With these and other capabilities, LiquidO has the potential to unlock new opportunities in neutrino physics, some of which are discussed here.

*Contact: anatae1@in2p3.fr and suekane@awa.tohoku.ac.jp.

†Also at Observatório Nacional, Rio de Janeiro, Brasil

‡Deceased.

§Blaise Paschal Chaire Fellow.

The discovery of the neutrino (ν) in the fifties [1] revolutionised particle physics not only by establishing the existence of this elusive particle, but also by laying the groundwork for a technology at the basis of many subsequent breakthroughs and whose use has extended beyond ν physics. The liquid scintillator detector (LSD) developed by Cowan, Reines et al. for ν detection exploited a well established radiation detection technique at the time, whereby molecular electrons are excited by the passage of charged particles produced by ν interactions and then emit light upon de-excitation [2]. This light is detected by sensitive photon detectors, typically photomultiplier tubes (PMTs) [3], that surround the scintillator volume and are often located many metres from the interaction point. Cowan, Reines et al. relied on the *inverse- β decay* (IBD) reaction, given by $\bar{\nu}_e + p \rightarrow e^+ + n$, that yields two clear signals: the prompt energy deposition of the e^+ (including annihilation γ 's) followed by the nuclear capture signal of the n after thermalisation. The close time and space coincidence between these two was exploited as the primary handle to separate the signal from the background (BG). The simplicity and power of this technique, enabled in great part by the abundant light produced by the scintillators, has allowed LSDs to dominate several areas of neutrino physics, particularly at the lower part of the MeV energy scale.

Despite their many advantages, LSDs have limitations. The propagation of light through the scintillator itself makes transparency an essential requirement for efficient light collection, potentially limiting the size of the detector volume. Given the extremely small probability for neutrinos to interact with matter, achieving larger detectors has in fact been a standing challenge throughout the history of ν physics. LSDs have gone from a few hundred kilograms, at the time of Cowan, Reines et al., to today's 20 kilotons with JUNO [4], where a record setting mean attenuation length of greater than 20 m is foreseen. The need for transparency has also set tight constraints on the type and concentration of elements that can be loaded into the scintillator. The physics goals of certain experiments call for detector doping [5], where an element other than the scintillator's native H and C is added to enhance detection capabilities or to search for rare processes. The discovery of the neutrino itself involved doping the detector with ^{113}Cd [6] to increase the energy released on n capture and thus further reduce the BG. However, to this day, doping in LSDs has been limited at high concentrations by transparency and stability constraints.

LSDs are also known to have a rather poor event-by-event topological discrimination power. It is essentially impossible to distinguish an individual e^+ from a e^- or a γ below 10 MeV, and it is even very difficult to tell whether one or several events have occurred simultaneously. The primary approach to deal with these limitations has been to segment the detector. Here the main volume is subdivided into optically-decoupled compartments, so instead of a single monolithic volume a granular one is used. This allows recovery of topological information from each neutrino interaction, i.e. images of the space and time pattern of an event, and hence enhances a detector's *event identification* capability. This technique has been very successfully used with GeV-scale neutrinos, where the large physical extent of the events allows imaging of

the final state particles using segmentation of a few centimetres. The largest example today is the 14 kiloton NOvA detector [7, 8], where the resulting images of the neutrino events are crucial for BG rejection and identification of different types of neutrino interactions. The situation is more difficult with MeV-scale neutrino interactions given the smaller physical extent of the resulting energy depositions, although there can still be advantages. For instance, the coarsely segmented detector introduced by Cowan, Reines et al. [1] exploited the unique anti-matter annihilation pattern of the e^+ , producing two back-to-back mono-energetic γ 's, as an aid to event identification. It is difficult however to segment finely enough to resolve the full topological information of individual events at these low energies without introducing certain disadvantages, such as dead material, radioactivity, cost, etc.

In addition to segmentation and doping, Cowan, Reines et al. also pioneered the use of two additional handles that are still widely relied upon to enhance signal to background separation in LSDs: a) detector shielding and b) signal modulation. Shielding was achieved by placing the detector underground and surrounding it with lead, thus reducing the cosmogenic¹ and radiogenic² BG, respectively. Signal modulation was possible via the reactor on/off periods, but this is generally impossible with natural ν sources.

Much of today's state of the art in ν detection owes directly to the work of Cowan, Reines et al. Numerous discoveries have been made since using ν 's from reactors, the sun, the interaction of cosmic rays in the atmosphere, accelerator produced beams, one supernova explosion (SN1987A), the earth and other astrophysical sources [9], and LSDs have played key roles in many of them. Despite the remarkable progress, the limitations of today's detector technology constrain our ability to probe the ν beyond our current knowledge and to use it in further exploring the universe. The approach presented here, called LiquidO, was designed to build on the strengths of the existing technology while also giving rise to unprecedented capabilities, such as high-resolution imaging and a more natural affinity for doping. The result is an innovative detector concept with the potential to break new ground in various frontiers of neutrino physics, some of which have remained elusive for decades.

LiquidO's Novel Detection Technique

The LiquidO technique is based on using opaque scintillator. Opacity can be achieved in two ways, through light scattering and/or absorption. The LiquidO approach relies on a very short scattering length and an intermediate absorption length, producing a scintillator that is milky and translucent in appearance. Photons from the scintillator undergo a random walk about their origin, giving rise to *stochastic light confinement*. While the path of each photon is stochastic, the integral effect is the confinement of the light to a sphere around each ionisation point, resulting in the production of so-called *light-balls*. This is the principle at the heart of the LiquidO technique.

¹Those caused by cosmic rays (mainly μ) directly or indirectly.

²Those caused by natural radioactivity, mainly α , γ or β^- .

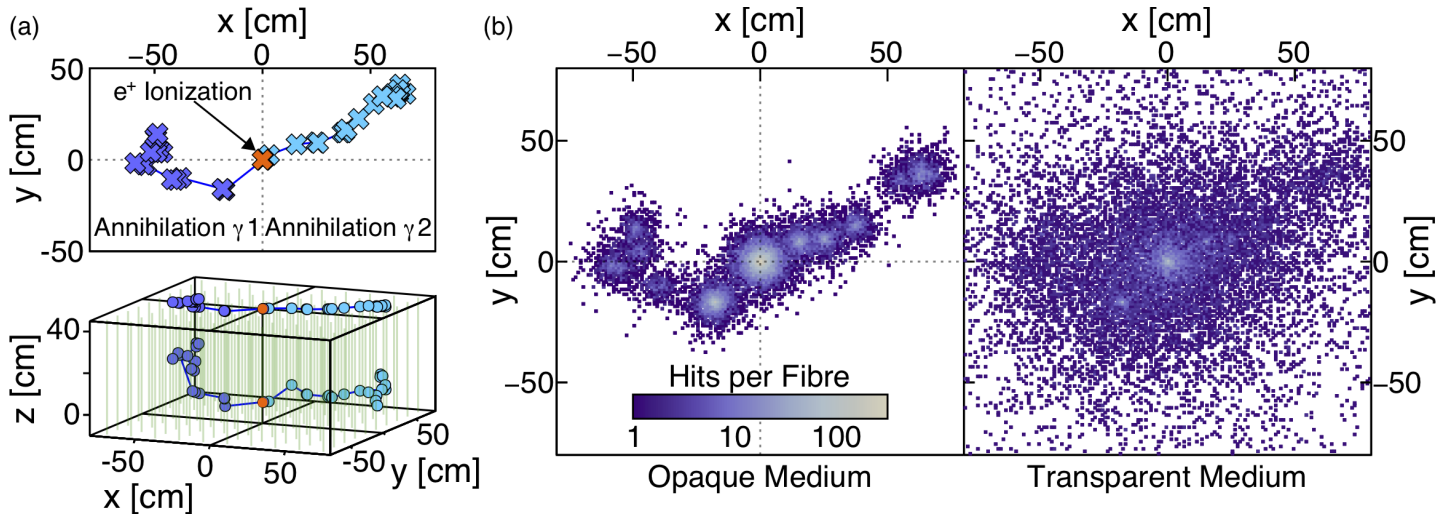


Figure 1: LiquidO Detection Principle and Imaging Capability. The energy deposition of a simulated 1 MeV positron in a LiquidO detector is used to illustrate the detection principle and imaging capability. The simplest configuration of detector geometry is shown in (a). The bottom diagram shows how the green fibres run through the scintillator in parallel with the z -axis and the top plot shows the x - y projection. The energy deposition of the positron is shown by the red point and the Compton scatters of the 0.51 MeV back-to-back annihilation γ 's by light and dark blues. One of the γ 's (dark blue) turns upwards to run approximately parallel with the fibres and this is reflected by its shorter extent in the x - y projection. In (b) the simulation of the light hitting each fibre in a 1-cm-pitch lattice is shown in two scenarios. On the left an opaque scintillator with a 5 mm scattering length is simulated whereas on the right the scintillator is transparent. The colour of each point represents the number of photons hitting a fibre at that x - y location. With a transparent medium the resulting image from the fibre array is almost completely washed out. In stark contrast, the light confinement around each energy deposition with the opaque scintillator allows preservation of the event's precious topological information and the formation of a high-resolution image.

Scintillators used in modern neutrino experiments typically have scattering lengths of up to tens of metres. Reducing the scattering length down to the scale of millimetres causes the light to be confined to a volume that is much smaller than the typical physical extent of, for example, a 1 MeV γ -ray event whose energy is lost via Compton scattering. To extract the light a lattice of wavelength-shifting fibres runs through the scintillator. With a lattice spacing on the scale of a centimetre, prompt and efficient light collection can be achieved and absorption losses minimised. Many configurations of the fibre lattice are possible, and in principle fibres could run in all three orthogonal directions. In practice, fibres running in only one direction might suffice for most purposes.

Fig. 1(a) illustrates the detection principle using the simplest configuration where the fibres all run along the z -axis. The energy depositions from a simulated 1 MeV e^+ are shown. The light captured by the fibres forms a two-dimensional (x , y) projection of the ionisation pattern, which is shown in the top plot of Fig. 1(a). Furthermore, by considering the difference in time of the light detection at the two ends of each fibre, information about the position of light capture along the length (z -coordinate) can be extracted. Fig. 1(b) shows a simulation of the simple detector configuration where the colour of each point shows the number of photons hitting a fibre. On the left an opaque scintillator is simulated and on the right the scintillator is transparent. The formation of the light-ball around the position of each Compton electron can be seen clearly for the opaque scintillator, whereas that pattern is almost completely washed out in the transparent case.

Previous scintillator detectors aiming to address the MeV e^+ topology have required fine segmentation. In contrast, the LiquidO technique effectively self-segments due to stochastic light confinement. This eliminates the need to add dead material (with associated potential radioactivity) to achieve segmentation and therefore substantially reduces the cost and complexity of producing scintillator detectors capable of high-resolution imaging.

The development of the LiquidO approach builds on much of the well-established technology of scintillator detectors, including modern Si-based photo-sensors (SiPM) [10, 11], wavelength shifting fibres and the organic scintillator materials themselves. The scintillator's stable isotopes, consisting mainly of H and ^{12}C (98.9% natural abundance), are well documented as neutrino interaction targets. The SiPMs have high quantum efficiencies of 50% and fast-time resolutions of up to 100 ps per photon detected [12]. From our simulations, it is estimated that more than 90% (60%) of the light will hit the fibres of a 1-cm-pitch lattice in a scintillator with an absorption length of 5 m (1 m). Compared to the tens of metre long absorption lengths necessary for the largest LSD based experiments, this represents a substantial reduction in the requirements for transparency. With a typical organic scintillator light yield of about 10 photons per keV [2], and a wavelength shifting fibre acceptance of about 10% (the main loss in detection [13]), the number of detected photons is estimated to be a maximum of around 300 per MeV for LiquidO. When scaling to larger detectors this amount will reduce due to the several-metre attenuation lengths typical

of wavelength-shifting fibres. Less conventional scintillator strategies could also work in LiquidO, such as water-based liquid scintillators [14] and other scintillators that would not be deemed transparent enough for traditional LSDs. Exceptional levels of scintillator radio-purity are possible, as has been demonstrated by the Borexino experiment [15]. The presence of fibres in the scintillator volume is mitigated by the fact that they typically amount to less than 1% of the detector mass fraction and that excellent levels of radiopurity have been achieved [16]. For physics measurements requiring extremely low backgrounds from natural radioactivity (at energies below 3 MeV), further improvements in fibre radiopurity may be necessary.

The main advantage of LiquidO is that its imaging capabilities, in combination with the properties of organic scintillators, allow for the discrimination of individual e^+ , e^- and γ events. The top panels of Fig. 2 show a comparison of the topology of an e^- and a γ at 2 MeV. The e^- deposits all its energy within a centimetre whereas the γ Compton scatters over many tens of centimetres. The discrimination power of LiquidO is quantified in the bottom plot of Fig. 2 where the probability that a γ is misidentified as an e^- is shown versus the electron selection efficiency. The results of these studies indicate that e^- 's can be feasibly distinguished from γ 's in LiquidO with a contamination factor of only 10^{-3} . Similarly, the topology of a e^+ annihilation event, with its back-to-back γ 's as illustrated in Fig. 1, stands in stark contrast to the point-like energy deposition of an e^- .

Much of this differentiation stems from the scintillator's low density, typically 0.9 g/cm^3 , and its high fraction of hydrogen with H-to-C ratios typically in the range 2-3. Its low average atomic number favours a long radiation length, around 0.5 m , a minimal photo-electric effect and energy losses by bremsstrahlung that do not start to dominate until electrons have an energy of around 100 MeV . The extremely low cross-section for the photo-electric effect in scintillator, such as Linear-Alkylbenzene (LAB) [17], means that an MeV-scale γ is highly unlikely to interact that way. On the rare occasion that this does happen an e^- of the same energy is produced, which sets a limit to the level at which e^- 's and γ 's can be distinguished. In scintillator the fraction of 2 MeV γ 's that interact via the photo-electric effect (the photofraction) is only 6×10^{-6} whereas in a heavy liquid such as xenon it is 2.9%. Doping a scintillator with a metal causes the photofraction to increase. For example, if indium at 10% by mass is used the photofraction rises to 0.17%. These numbers are illustrated in the bottom right of Fig. 2, allowing comparison of the probability of the event reconstruction misidentifying a γ as an e^- with the floor to performance set by the detector material.

Studies of the imaging capabilities of a detector with a 1-cm-pitch lattice indicate that the position of a 1 MeV e^- could be reconstructed to a precision of a few millimetres, which is an order of magnitude better than a typical LSD. Moreover, the light in the scintillator spreads out from a point source at up to $1/10 \times$ the speed of light due to scattering. This suggests that the consideration of both time and position information could enhance the discrimination of particle types with distinct *energy-flow* patterns such as e^+ and γ 's. Work

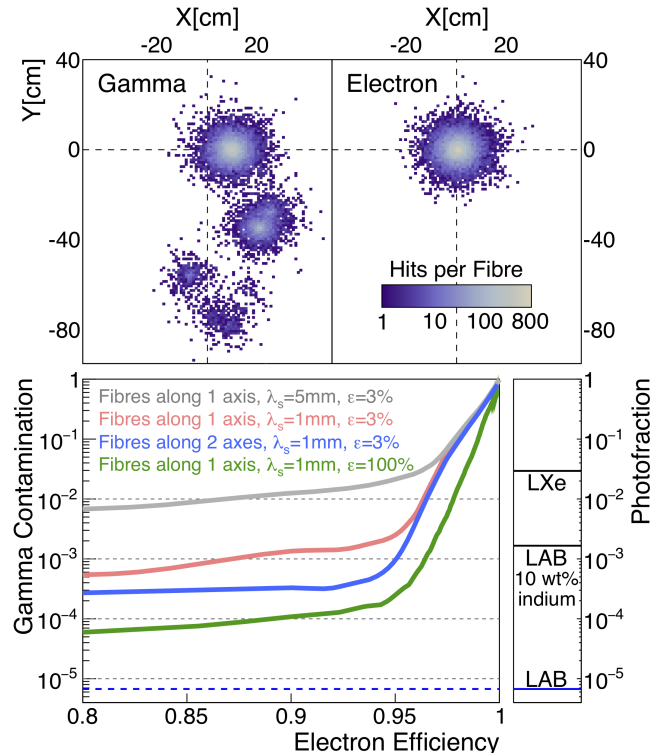


Figure 2: **LiquidO Discrimination of Electrons from Gammas.** The top two plots show a simulated γ (left) and e^- (right) at 2 MeV in the LiquidO detector of Fig. 1. The spatially dispersed Compton-scattering pattern of the γ clearly sets it apart from the e^- . A lower limit to the discrimination capability of a material is set by its photofraction, which is the fraction of γ 's that interact via the photo-electric effect. When this occurs, the γ transfers all its energy to an e^- and the two become indistinguishable. LAB has a remarkable photofraction of 6×10^{-6} , compared to 2.9% for liquid xenon and 0.17% for LAB doped with 10% indium by weight. The bottom plot shows the probability of misidentifying a γ as an e^- vs. the efficiency of selecting electrons estimated with a simple reconstruction, along with a photofraction scale on the right that shows the floor to detector performance. The red curve represents a baseline scenario using components with well-established performance. The LAB scintillator is assumed to have a conventional light yield and a mean scattering length λ_s of 1 mm, which is well-matched to the 1 cm fibre pitch. The photon detection efficiency ϵ of 3% accounts for all losses of light at the various stages and is dominated by the fibre trapping efficiency (around 10%) and the SiPM quantum efficiency (around 50%). In this baseline scenario, the probability of misidentifying a 2 MeV γ as an e^- is estimated to be at the 10^{-3} level. The grey curve illustrates how the probability of misidentifying γ 's increases when light is not confined tightly enough ($\lambda_s=5 \text{ mm}$). The blue curve shows the improvement relative to the baseline that can be obtained when fibres with the same 1 cm pitch run along 2 orthogonal axes instead of a single one. Finally, the green curve illustrates how much hypothetical improvement could be obtained with a large $30 \times$ more light, some of which might be achieved through novel scintillators and/or improved photon detection efficiency. No timing information has been used and more sophisticated spatial reconstruction techniques could likely improve the e^- vs. γ separation further.

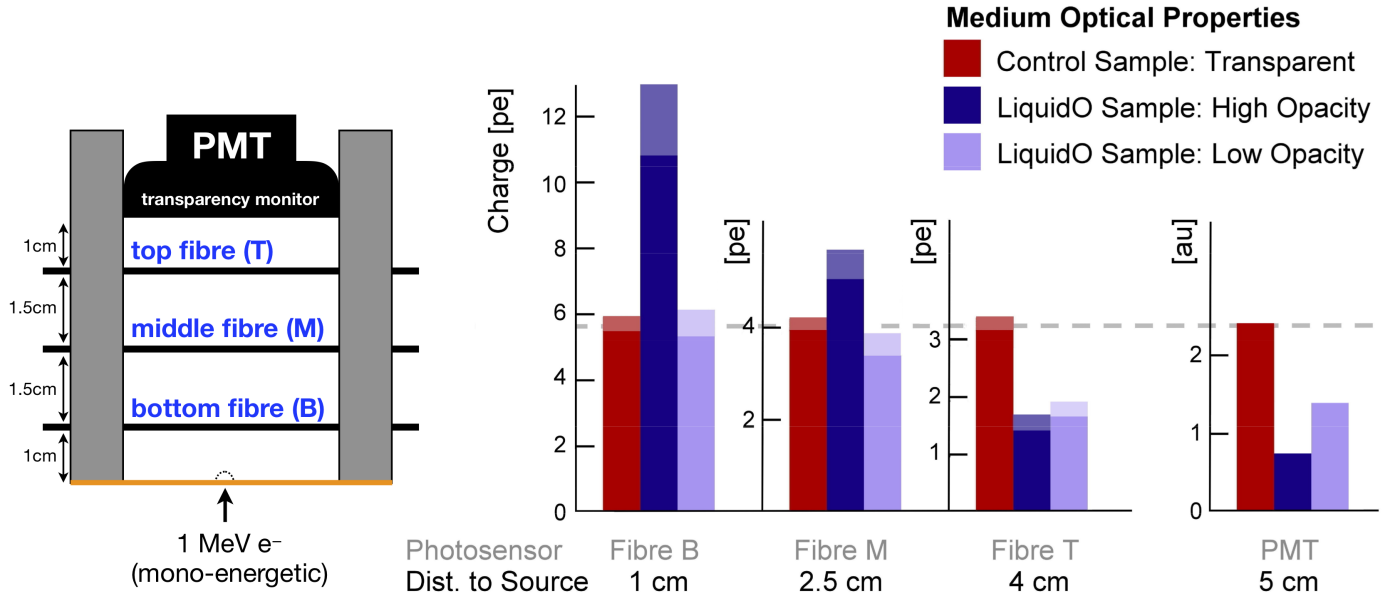


Figure 3: LiquidO Experimental Proof of Principle. The left panel shows a diagram of the small prototype detector built for the first experimental demonstration of LiquidO’s detection principle. The detector consists of a small cylindrical vessel with internally reflecting surfaces including a $25 \mu\text{m}$ aluminised Kapton sheet at the bottom. Light is collected with three fibres ($\phi=1 \text{ mm}$) running diametrically at different heights. A 3” PMT is placed at the top and serves as a transparency monitor. Mono-energetic $1 \text{ MeV } e^-$ ’s impinge from the bottom and make point-like energy depositions inside the detector as shown by the dashed semi-circular line. The data collected with three scintillators made from the same base (LAB+PPO at 2 g/l) are shown on the right with measurement uncertainties illustrated by the pale regions at the top of each bar. The high (dark blue) and low (light blue) opacity formulations are obtained by mixing in a paraffin polymer at 10% and setting the temperature at 12°C and 26°C , respectively. Studies of an LAB-based scintillator showed only percent-level effects on the light yield from a similar temperature change [18]. The measurements from the prototype obtained with the opaque formulations are compared with those from the transparent scintillator (red), which serves as a control sample. To allow relative changes in light collection between the three fibres and the PMT to be seen easily, the axes of each bar chart were scaled so that the red bars are all the same height (grey dashed line). The high opacity data show a clear increase (around $2.0\times$) at the bottom of the vessel and a decrease (around $0.5\times$) at the top, as expected from stochastic light confinement around the energy deposition point. Given that the low and high opacity samples have the same composition and differ only in temperature, these results show that the formation of a light-ball and the corresponding increase in light collection at the bottom fibre are directly linked to the shorter scattering length.

is ongoing to assess LiquidO’s capability to perform dynamic imaging of energy deposition in time and its improvement over the static imaging used in Fig. 2.

Particles such as muons would leave clear track signatures in a LiquidO detector as sequences of point-like energy depositions. The expected millimetre precision tracking could allow many cosmogenically-induced radioisotopes to be actively tagged and reduced with high efficiency and a small impact on detector exposure. Also, the tenfold quenching of light production [2] from the high density ionisation of a MeV-scale alpha or proton helps reduce those backgrounds to identifying e^+ , e^- and γ particles above 1 MeV. The longer light emission profile (i.e. longer tail) from high density ionisation allows pulse shape discrimination [19] of particles with different masses, such as e^- , α and p^+ , with suitable scintillator formulations.

A particularly promising avenue for exploiting the LiquidO approach is where doping of the scintillator opens up the possibility of new physics measurements. One of the major challenges usually associated with doping LSDs is maintaining the optical properties, including transparency, while achieving the desired concentration of the dopant. In con-

trast, the LiquidO technique actually requires opacity to confine the light and therefore allows for consideration of more possibilities, be it to load new materials or to achieve higher levels of doping. Examples of what can be achieved with a doped scintillator are wide and varied. The original Cowan, Reines et al. experiment used cadmium to efficiently detect neutrons and the LENS experiment concept involved using an indium-doped liquid scintillator [20, 21, 22]. Several neutrino-less double beta decay experiments use or propose doped scintillators [23, 24, 25, 26] as the way forward to realise higher isotopic masses. The strong precedent set by LENS with indium suggests that loading at more than 10% for neutrino-less double beta decay searches is a reachable objective.

First Experimental Proof of Principle

An experimental proof of principle for LiquidO has been successfully completed with a small detector prototype. The setup focused on demonstrating the primary feature of LiquidO, which is the stochastic confinement of light. The test was done with point-like e^- energy depositions to demonstrate the formation of the characteristic light-ball.

Well-established technological solutions were used in the prototype for both the readout and the scintillator base. The latter was formulated from transparent LAB with a PPO wavelength-shifter at 2 g/l. The opacity was obtained in a novel way by mixing in a paraffin polymer at 10% to give a uniform, waxy consistency [27]. Like in many waxes, the resulting scintillator was observed to transition from a transparent liquid phase at $>30^\circ\text{C}$ to an opaque white solid phase at $<15^\circ\text{C}$. This temperature dependence was exploited in the demonstration, as explained below. The scintillator was poured into a prototype detector that consisted of a small (0.25 litre and 5.0 cm height) cylindrical vessel with internally reflecting surfaces. Three identical Kuraray B-3 wavelength-shifting fibres were run along diametrical lines at different heights, as shown schematically on the left of Fig. 3, and read out with Hamamatsu S12572-050 SiPMs. The detector was exposed to a mono-energetic 1 MeV e^- source [28] impinging from the bottom through a thin 25 μm aluminised Kapton sheet. The e^- 's deposited their energy in the first few millimetres of scintillator.

The results from the prototype are shown on the right of Fig. 3. Three scintillator configurations were utilised: transparent (no added polymer), low opacity and high opacity. The former was a control sample and the latter two were obtained by varying the temperature of the same sample of opaque scintillator. Direct comparison of the relative fibre response between the transparent and opaque scintillators allowed common systematic uncertainties to cancel, making the use of simulation unnecessary. In the transparent case, the PMT saw the most light and the fibres saw different light levels consistent with their respective solid angle acceptance as the dominant effect. When the opaque scintillator was used the light seen by the PMT and the top fibre was predictably reduced by a large factor. This light was not simply lost. The remarkable increase in light collection by the middle and bottom fibres ruled out an absorption-only scenario and showed that the light was stochastically confined around the point-like energy deposition at the bottom. The measurements at different heights sampled the longitudinal profile of the corresponding light-ball, confirming the LiquidO detection principle.

An interesting byproduct of this measurement was the observation of temperature controlled solidification of the waxy material. This could open the door to several possibilities, such as doping scenarios not bound by chemical stability constraints. The solidification also grants additional mechanical support for the fibre lattice and protection against leaks.

Neutrino Physics with LiquidO

The LiquidO approach opens up enhanced neutrino detection potential via several avenues and likely beyond, be it the search for proton decay [29] or neutrino-less double beta decay [30], calorimetry in high-energy physics or applications in radiation detection. In this paper, we focus on possible measurements of neutrinos at the MeV-scale. This energy range alone provides a rich landscape of challenging physics with discovery potential, addressing both the nature of the neu-

trino and some key neutrino sources such as the earth [31], the sun [32] and supernovae [33]. While geoneutrinos and solar neutrinos constitute unique, direct probes of the heat budget of the planet and stellar physics respectively, supernovae neutrinos would shed unique insight into star collapse processes where heavy elements are forged. The neutrino itself is believed to hold access to answering compelling questions about the formation and evolution of our universe, which could be addressed by elucidating the properties of the neutrino such as absolute mass scale, CP-violation and resolution to the puzzle of whether a ν is its own anti-particle. In the following sections, we briefly illustrate a few examples where it is reasonable to expect LiquidO to have breakthrough potential.

Physics Potential with Anti-Neutrinos. We begin the discussion with a direct comparison of the LSD and LiquidO techniques in the context of measuring reactor $\bar{\nu}_e$'s. This source continues to enable important measurements in neutrino physics, such as the precision determination of neutrino oscillation parameters and searches for new physics states or interactions beyond the Standard Model, among others. The LiquidO technique is also directly relevant to the detection of anti-neutrinos from other sources, such as supernovae and the earth, as well as from pion decay-at-rest beams [34, 35].

As previously mentioned, $\bar{\nu}_e$'s above 1.8 MeV can produce an IBD interaction with the resulting event being a e^+ and n pair as the observable. The close coincidence in time and space between the e^+ and n is the main handle for background rejection with most LSDs.

Up to now, current LSDs have two limitations with regards to identifying IBD events. First, single e^+ events are largely indistinguishable from e^- 's and γ 's with the same visible energy. Second, although the neutron coincidence is useful, neutron backgrounds tend to be copious. In particular, cosmogenic production of neutrons – sometimes even preceded by β^- decays – can produce backgrounds to IBD events. In contrast, the unique signature of a e^+ event in a LiquidO detector, as shown in Fig. 1, provides a new and powerful handle that could be used to reject both cosmogenic and accidental backgrounds. As shown in Fig. 2, electrons or other particles giving point-like energy deposition are estimated to be misidentified as a γ with probability of at most 10^{-2} , which gives an upper limit on the probability of misidentifying them as a e^+ . Thus, all cosmogenic backgrounds whose final states consist of e^- , α or recoil- p can be reduced by a factor of at least a hundred in comparison to the latest LSDs [36]. The accidental backgrounds involving a β^- can be similarly rejected from the prompt e^+ signals. Any remaining accidental backgrounds dominated by γ 's can be reduced by both the event identification capability to discriminate between e^+ and γ 's and the spatial coincidence requirement that can be tightened by the more precise mm-scale vertex reconstruction. On top of those BG reductions, a decrease in the radioactivity present within the detector is possible through the elimination of the need for PMTs in the LiquidO approach. As an example, the overall signal to background ratio of the Double Chooz near detector [36], with an overburden of barely 30 m of rock, would be reasonably expected to increase by two orders of magnitude, from about 20 to order 1000.

IBD detection where backgrounds are hugely reduced opens the door to new explorations, such as a reactor anti-neutrino oscillation measurement beyond today’s precision. In situations where a high signal-to-background ratio was unnecessary, a major reduction of the overburden requirement might become possible, as low-background performance can be envisaged closer to the surface thanks to the detector’s native background rejection. This makes LiquidO an ideal detector to monitor reactor anti-neutrinos for non-proliferation purposes [37]. LiquidO’s opacity and fibre-lattice readout also allows for a much more efficient use of precious underground laboratory space. In LSDs, a passive “buffer” region is often used to shield against PMT or other radioactivity, and has been up to about $4\times$ larger in volume [36] than the neutrino target in past experiments. This buffer is necessary for a monolithic detector since light from energy deposited anywhere in the central region can in principle be seen by all the photo-sensors. In contrast, for a detector like LiquidO that self-segments into many optically-decoupled regions, this buffer is no longer a crucial design feature and can be greatly reduced or removed.

LiquidO’s single- e^+ identification capabilities also open a door to new or complementary modes of $\bar{\nu}_e$ detection that were previously inaccessible. New target isotopes could potentially enable exploration of the region below the 1.8 MeV IBD threshold for the first time. Control of cosmogenic e^+ backgrounds would be necessary and LiquidO’s high-resolution imaging could help significantly with that. One example is the β^+ decay of the cosmogenic ^{11}C production ($\tau \approx 20$ minutes) that could be reduced via spatial correlation to the precisely tracked progenitor muon.

Physics Potential with Neutrinos. The detection of MeV-scale electron neutrinos (ν_e) is in general a much greater challenge than that for $\bar{\nu}_e$ in LSDs. A ν_e charged current (CC) interaction produces an e^- in the same way a $\bar{\nu}_e$ produces a e^+ , but measuring those e^- ’s is extremely hard due to the indistinguishable β^- from natural radioactivity. It has, however, been done by experiments that went to enormous efforts to improve the radio-purity of their detection volumes [15]. Another major issue is that there is no ν_e CC interaction on pure organic scintillators below 15 MeV with a high-enough yield to be useful, except for elastic scattering with electrons. The LiquidO technique combined with using a dopant could enable new measurements of electron neutrinos from sources that include the sun, supernovae and pion decay-at-rest beams.

In 1976 the possibility of doping with indium to enable MeV-scale ν_e CC interactions in a detector was proposed by Raghavan [38]. The interaction is $\nu_e + ^{115}\text{In} \rightarrow e^- + ^{115}\text{Sn}^*$ and has a threshold of only 114 keV. The energy of the e^- is proportional to that of the incoming ν_e and the excited tin nucleus decays in delayed coincidence with $\tau = 4.76 \mu\text{s}$. The tin decay produces a 497 keV γ along with either a γ or e^- at 116 keV. Simulated images of these two tin decays in a LiquidO detector are shown in Fig. 4. Indium is 95.7% ^{115}In and it has been shown that stable scintillators with up to 10% indium by weight can be achieved [20, 21]. The signature of the ν_e interaction on indium in a LiquidO detector

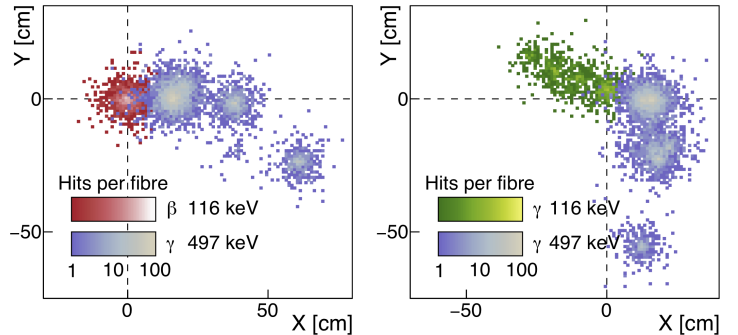


Figure 4: Combining LiquidO with ^{115}In to Enable New Measurements of Electron Neutrinos. At an energy of greater than 128 keV electron neutrinos undergo a charged current interaction on ^{115}In , which could be added as a dopant at high concentrations to a LiquidO detector. The e^- produced has an energy proportional to the original neutrino and the excited $^{115}\text{Sn}^*$ nucleus decays in delayed-coincidence with $\tau = 4.76 \mu\text{s}$. The two plots show a LiquidO simulation of the number of photons hitting each fibre in a 1-cm-pitch lattice for the two possible decay modes of $^{115}\text{Sn}^*$. In both cases a 497 keV γ is produced together with either an e^- (left) or a γ (right) at 116 keV. The colour of each point represents the number of photons hitting a fibre at that x-y location. The energy deposit of the prompt e^- is not shown in the plots but provides the time and space coordinates to look for the mono-energetic tin decay in delayed-coincidence. Furthermore, the high-resolution images enable efficient background rejection by requiring a point-like energy deposition of the e^- to be followed by the spatially dispersed Compton-scattering pattern of a γ . This distinct signature that arises from combining indium with a LiquidO detector exemplifies the potential of the technique.

is powerfully distinct. The prompt e^- provides the time and space coordinates to look for the mono-energetic tin decay in delayed coincidence. Furthermore, the high-resolution images enable efficient background rejection by requiring a point-like energy deposition of the e^- to be followed by the spatially dispersed Compton-scattering pattern of a γ . Should the rejection power be large enough to address the intrinsic ^{115}In β^- decay ($Q = 497$ keV, $\tau = 6 \times 10^{14}$ years) then even neutrinos from the main solar fusion chain (99.5% of the flux) might be within reach, as was originally envisaged.

Many possibilities for other dopants can be considered. To detect higher energy neutrinos other isotopes are known [39], such as ^{208}Pb that has a higher cross-section than the ^{12}C present in organic scintillators [40, 41]. Both ^{208}Pb and ^{12}C also grant neutrino flavour independent (ν_x) detection, via neutral current interactions. A LiquidO detector doped with ^{208}Pb at high concentrations would potentially enable simultaneous detection and identification of the ν_e , $\bar{\nu}_e$ and ν_x channels. Choosing the level of doping is an optimisation that depends on the physics goals and various detector parameters. For example, the ability of a LiquidO scintillator detector to discriminate particles with point-like energy depositions from γ ’s, as shown in Fig. 2, is intrinsically reduced in the presence of heavy metals.

In general, a LiquidO detector with the capability to measure ν_e ’s and $\bar{\nu}_e$ ’s simultaneously would be ideal for sources that are an unavoidable mixture of both neutrinos and an-

tineutrinos. A low threshold measurement of the flux from a supernova of both ν_e and $\bar{\nu}_e$ separately would be possible. Another example is a pion decay-at-rest beam where a mixture of primarily three types of neutrinos, ν_μ , $\bar{\nu}_\mu$ and ν_e , are produced. The ability to identify each type separately opens up new opportunities to measure leptonic CP-violation [42] or other sub-dominant transitions.

Conclusions

The LiquidO detection technique is described here for the first time. This novel technology builds upon decades of existing expertise using scintillator detectors, but departs from the dominant transparency-based approach by exploiting an opaque scintillator medium. With a short scattering length, light is stochastically confined near its creation point, a behaviour that has now been successfully demonstrated in the laboratory. The result is a detector that preserves the advantages of conventional liquid scintillator detectors while adding detailed imaging of particle interaction topology that enables individual events to be identified. Additionally, LiquidO's unparalleled capacity for elemental doping is expected to facilitate new searches for rare processes and measurements of neutrinos, going beyond the interactions on H and C in organic scintillators. With the powerful background rejection capability offered by LiquidO and the possibility of loading suitable dopants at high concentrations, a wide panorama of opportunities becomes available in MeV-scale neutrino physics and beyond. Current work focuses on further exploring the physics capabilities while completing an R&D program towards concrete experimental scenarios.

Acknowledgements

We acknowledge the pivotal support received from the following grants: i) the Marie Curie Research Grants Scheme (Grant 707918 between 2016-2018, fellow: Dr. M. Grassi hosted by Dr. A. Cabrera at IN2P3/CNRS) that allowed the main studies behind the simulation proof-of-principle of LiquidO; ii) the ‘‘Chaire Internationale de Recherche Blaise Pascal’’ between 2016-2018 (Laureate: Prof. F. Suekane) financed by R egion Ile-de-France (Paris, France) and coordinated by the Fondation de l’Ecole Normale Sup erieure (Paris) and the IN2P3/CNRS via the APC Laboratory (Paris) that provided multiple levels of resources for the prototyping of LiquidO; and iii) the France-Japan Particle Physics Laboratory grant, since 2018, for fundamental research in particle physics cooperation between France and Japan. We are also very thankful to FONDECYT in Chile, CNPq and FAPERJ in Brazil, CNRS/IN2P3 in France, CIEMAT in Spain and the University of California at Irvine in USA for their generous provision of manpower and resources. We would like to acknowledge the support of the CENBG and the SuperNEMO collaboration for the use of their e^- beam for the LiquidO detector prototypes. Finally, we would like to thank several people whose knowledgeable input and kind assistance were instrumental to this publication. These are (alphabetically): Dr. F. Mauger, Prof. Dr. M. Lindner and Dr. Y. Lemi ere.

References

- [1] C. L. Cowan, F. Reines, F. B. Harrison, H. W. Kruse, and A. D. McGuire. Detection of the free neutrino: A Confirmation. *Science*, 124:103–104, 1956.
- [2] J. B. Birks. *The Theory and Practice of Scintillation Counting*. International Series of Monographs in Electronics and Instrumentation. Pergamon, 1964.
- [3] W. R. Leo. *Techniques for Nuclear and Particle Physics Experiments*. Springer-Verlag Berlin Heidelberg, 2 edition, 1994.
- [4] F. P. An et al. Neutrino Physics with JUNO. *J. Phys.*, G43(3):030401, 2016.
- [5] C. Buck and M. Yeh. Metal-loaded organic scintillators for neutrino physics. *J. Phys.*, G43(9):093001, 2016.
- [6] A.R. Ronzio, L. Cowan Jr., and F. Reines. Liquid Scintillators for Free Neutrino Detection. *Review of Scientific Instruments*, 29:146–147, 1958.
- [7] D. S. Ayres et al. The NOvA Technical Design Report. FERMILAB-DESIGN-2007-01, 2007.
- [8] M. A. Acero et al. New constraints on oscillation parameters from ν_e appearance and ν_μ disappearance in the NOvA experiment. *Phys. Rev.*, D98:032012, 2018.
- [9] M. Tanabashi et al. Review of Particle Physics. *Phys. Rev.*, D98(3):030001, 2018.
- [10] P. Buzhan et al. Silicon photomultiplier and its possible applications. *Nucl. Instrum. Meth.*, A504:48–52, 2003.
- [11] D. Renker. Geiger-mode avalanche photodiodes, history, properties and problems. *Nucl. Instrum. Meth.*, A567:48–56, 2006.
- [12] V. Puill et al. Single photoelectron timing resolution of SiPM as a function of the bias voltage, the wavelength and the temperature. *Nucl. Instrum. Meth.*, A695:354 – 358, 2012.
- [13] J. D. Weiss. Trapping efficiency of fluorescent optical fibers. *Optical Engineering*, 54(2):1 – 5, 2015.
- [14] M. Yeh et al. A new water-based liquid scintillator and potential applications. *Nucl. Instrum. Meth.*, A660:51–56, 2011.
- [15] C. Arpesella et al. Measurements of extremely low radioactivity levels in BOREXINO. *Astropart. Phys.*, 18:1–25, 2002.
- [16] M. Agostini et al. Upgrade for Phase II of the Gerda experiment. *Eur. Phys. J.*, C78(5):388, 2018.
- [17] M. C. Chen. The SNO liquid scintillator project. *Nucl. Phys. Proc. Suppl.*, 145:65–68, 2005.
- [18] A. S orensen et al. Temperature quenching in LAB based liquid scintillator. *Eur. Phys. J.*, C78(1):9, 2018.
- [19] G. Ranucci et al. Scintillation decay time and pulse shape discrimination of binary organic liquid scintillators for the Borexino detector. *Nucl. Instrum. Meth.*, A350:338–350, 1994.
- [20] N. A. Danilov et al. A Study of Indium Extraction with Carboxylic Acids with the Aim to Produce Scintillators for Solar Neutrino Detection by LENS Spectroscopy of Low-Energy Neutrino. *Radiochem.*, 47(5):487–493, 2005.
- [21] C. Grieb, J. Link, and R. S. Raghavan. Probing active to sterile neutrino oscillations in the LENS detector. *Phys. Rev.*, D75:093006, 2007.

- [22] C. Buck et al. Luminescent properties of a new In based organic liquid scintillation system. *J. Lumin*, 106:57–67, 2004.
- [23] A. Gando et al. Search for Majorana Neutrinos near the Inverted Mass Hierarchy Region with KamLAND-Zen. *Phys. Rev. Lett.*, 117(8):082503, 2016. [Addendum: *Phys. Rev. Lett.*117,no.10,109903(2016)].
- [24] S. Andringa et al. Current Status and Future Prospects of the SNO+ Experiment. *Adv. High Energy Phys.*, 2016:6194250, 2016.
- [25] J. Zhao, L. J. Wen, Y. F. Wang, and J. Cao. Physics potential of searching for $0\nu\beta\beta$ decays in JUNO. *Chin. Phys.*, C41(5):053001, 2017.
- [26] A. Cabrera. LiquidO: First Opaque Detector for $\beta\beta$ Decay? *PoS, NOW2018:028*, 2019.
- [27] C. Buck et al. Novel Opaque Scintillator for Neutrino Detection. Publication in preparation, 2019.
- [28] C. Marquet et al. High energy resolution electron beam spectrometer in the MeV range. *JINST*, 10(09):P09008, 2015.
- [29] P. Langacker. Grand Unified Theories and Proton Decay. *Phys. Rept.*, 72:185, 1981.
- [30] I. Shimizu and M. Chen. Double Beta Decay Experiments With Loaded Liquid Scintillator. *Front. Phys.*, 7:33, 2019.
- [31] O. Sramek, W. F. McDonough, and J. G. Learned. Geoneutrinos. *Adv. High Energy Phys.*, 2012:235686, 2012.
- [32] M. Agostini et al. Comprehensive measurement of pp -chain solar neutrinos. *Nature*, 562(7728):505–510, 2018.
- [33] K. Scholberg. Supernova Neutrino Detection. *Ann. Rev. Nucl. Part. Sci.*, 62:81–103, 2012.
- [34] A. Bolozdynya et al. Opportunities for Neutrino Physics at the Spallation Neutron Source: A White Paper. Preprint at FERMILAB-CONF-12-852-PPD, 2012.
- [35] M. Harada et al. Proposal: A Search for Sterile Neutrino at J-PARC Materials and Life Science Experimental Facility. Preprint at arXiv:1310.1437, 2013.
- [36] H. de Kerret et al. First Double Chooz θ_{13} Measurement via Total Neutron Capture Detection. Preprint at arXiv:1901.09445, 2019.
- [37] P. Huber and T. Schwetz. Precision spectroscopy with reactor anti-neutrinos. *Phys. Rev.*, D70:053011, 2004.
- [38] R. S. Raghavan. Inverse beta decay of 115-In to 115-Sn*: a new possibility for detecting solar neutrinos from the proton-proton reaction. *Phys. Rev. Lett.*, 37:259–262, 1976.
- [39] J. A. Formaggio and G. P. Zeller. From eV to EeV: Neutrino Cross Sections Across Energy Scales. *Rev. Mod. Phys.*, 84:1307–1341, 2012.
- [40] J. Engel, G. C. McLaughlin, and C. Volpe. What can be learned with a lead based supernova neutrino detector? *Phys. Rev.*, D67:013005, 2003.
- [41] C. Volpe, N. Auerbach, G. Colo, T. Suzuki, and N. Van Giai. Microscopic theories of neutrino C-12 reactions. *Phys. Rev.*, C62:015501, 2000.
- [42] M. Grassi, F. Pessina, A. Cabrera, S. Dusini, H. Nunokawa, and F. Suekane. Neutrino-Antineutrino Identification in a Liquid Scintillator Detector: Towards a Novel Decay-at-Rest-based Neutrino CPV Framework. *Nucl. Instrum. Meth.*, A936:561–562, 2019.